View Online / Journal Homepage / Table of Contents for this issue
Dynamic Article Links

PCCP

Cite this: *Phys. Chem. Chem. Phys.*, 2012, **14**, 9702–9714

www.rsc.org/pccp

PAPER

Direct aqueous photochemistry of isoprene high-NO_x secondary organic aerosol†

Tran B. Nguyen,[a] Alexander Laskin,[b] Julia Laskin[c] and Sergey A. Nizkorodov*[a]

Received 23rd March 2012, Accepted 17th May 2012
DOI: 10.1039/c2cp40944e

Published on 17 May 2012 on http://pubs.rsc.org | doi:10.1039/C2CP40944E
Downloaded by PNNL Technical Library on 25 June 2012

Secondary organic aerosol (SOA) generated from the high-NO_x photooxidation of isoprene was dissolved in water and irradiated with $\lambda > 290$ nm radiation to simulate direct photolytic processing of organics in atmospheric water droplets. High-resolution mass spectrometry was used to characterize the composition at four time intervals (0, 1, 2, and 4 h). Photolysis resulted in the decomposition of high molecular weight (MW) oligomers, reducing the average length of organics by 2 carbon units. The average molecular composition changed significantly after irradiation ($C_{12}H_{19}O_9N_{0.08} + h\nu \rightarrow C_{10}H_{16}O_8N_{0.40}$). Approximately 65% by count of SOA molecules decomposed during photolysis, accompanied by the formation of new products. An average of 30% of the organic mass was modified after 4 h of direct photolysis. In contrast, only a small fraction of the mass (<2%), belonging primarily to organic nitrates, decomposed in the absence of irradiation by hydrolysis. Furthermore, the concentration of aromatic compounds increased significantly during photolysis. Approximately 10% (lower limit) of photodegraded compounds and 50% (upper limit) of the photoproducts contain nitrogen. Organic nitrates and multifunctional oligomers were identified as compounds degraded by photolysis. Low-MW 0N (compounds with 0 nitrogen atoms in their structure) and 2N compounds were the dominant photoproducts. Fragmentation experiments using tandem mass spectrometry (MS^n, $n = 2$–3) indicate that the 2N products are likely heterocyclic/aromatic and are tentatively identified as furoxans. Although the exact mechanism is unclear, these 2N heterocyclic compounds are produced by reactions between photochemically-formed aqueous NO_x species and SOA organics.

1. Introduction

Atmospheric fog and cloud droplets are effective scavengers of water-soluble secondary organic aerosols (SOA) and volatile organic compounds (VOC).[1–5] The aqueous-phase processing in these systems is starting to be recognized as a key aging mechanism for atmospheric organic material (OM), with the most important abiotic processes initiated by sunlight. Photo-induced processing pathways for OM in cloud/fog water include *direct photolysis* where the organic compounds absorb radiation and undergo aqueous-phase chemical transformations, and *indirect photolysis* where solar radiation initiates chemistry through the production of non-selective oxidants like hydroxyl radical (OH) or through photosensitized energy transfers.[6,7] The non-photolytic fates of OM in cloud/fog droplets include hydrolysis[8,9] and evaporative processing with inorganic ions.[4,10–13]

Aqueous photoprocessing in general, including both direct and indirect photolysis, dramatically modifies the OM composition,[14,15] which alters the optical[16,17] and physical[18] properties of the OM. Direct and indirect photolysis occur simultaneously and their relative importance is highly dependent on atmospheric conditions (OM concentration, pH, inorganic ion concentration, radiation flux, and temperature) and the physico-chemical properties of the individual organic compounds (absorption cross section, photolysis quantum yield, and reactivity towards OH). For example, at pH > 4, the measured rates of direct and indirect photolysis of dinitrophenols in water are comparable, but indirect photolysis becomes more important at lower pH values.[19]

Much attention has been paid to the indirect aqueous photolysis of OM with the OH radical. The bulk of the research was focused on common water-soluble organic compounds including glyoxal and pyruvic acid, which produce high molecular weight (MW) oligomers when irradiated in the presence of H_2O_2 as an OH source.[14–16,20–28] Fewer articles focused on the photochemistry of complex mixtures,[18,29] such as irradiation of SOA extracts mixed with H_2O_2 generating

[a] *Department of Chemistry, University of California, Irvine, Irvine, California 92697, USA. E-mail: nizkorodo@uci.edu*
[b] *Environmental Molecular Sciences Laboratory, Pacific Northwest National Laboratory, Richland, Washington 99352, USA*
[c] *Chemical and Materials Sciences Division, Pacific Northwest National Laboratory, Richland, Washington 99352, USA*
† Electronic supplementary information (ESI) available. See DOI: 10.1039/c2cp40944e

This journal is © the Owner Societies 2012

Published on 17 May 2012 on http://pubs.rsc.org | doi:10.1039/C2CP40944E
Downloaded by PNNL Technical Library on 25 June 2012

highly-oxidized compounds. As aqueous photochemistry is highly matrix-dependent, studying complex aqueous mixtures such as dissolved SOA is more representative of atmospheric cloud and fog chemistry, although it will lead to dramatically greater complexity in the product distribution. However, chemical analysis of such mixtures is possible using advanced separation and/or high resolution mass spectrometry techniques (HR-MS).[30,31]

In cloud and fog water, the overall concentration of multi-component dissolved OM is considerably higher than the concentrations of individual organic compounds, which are typically in the 10^{-12}–10^{-6} M range. Measured OM concentrations approach 200 μg mL^{-1} in some locations (or up to 10^{-3} M assuming a molecular weight of 200 g mol^{-1} for a typical OM compound).[32–40] In smaller aqueous droplets or in polluted areas, $[OM]_{dissolved}$ can be high and the oxidative capacity of OH may be too low to oxidize all dissolved organics during the droplet lifetime. Furthermore, higher OM concentrations have also been shown to suppress photochemical OH production,[41] sometimes diminishing the importance of OH-initiated chemistry almost entirely without significantly perturbing the efficiency of direct photolysis for photolabile compounds.[42]

Sparse literature is available on direct aqueous photolysis of atmospherically-relevant OM even though many abundant water-soluble OM compounds, *e.g.*, organic nitrates and carbonyls, are readily affected by direct photolysis due to their significant absorption cross sections in the actinic wavelengths.[43–52] Furthermore, organic nitrates with a neighboring carbonyl group, which are relevant to SOA, have enhanced absorption cross sections in the near UV wavelengths.[44,45] Previously, the effect of direct aqueous irradiation on OM composition has been studied only for pyruvic acid,[27] phenols,[53] and extracts of limonene/ozone SOA.[54] These direct photolysis studies can result in either a net gain or loss in high-MW species, depending if the experiments focused on single compounds or SOA mixtures, again underscoring the dramatic matrix effects.

Direct photolysis rates can be estimated for carbonyls in aqueous extracts of biogenic SOA ($J \sim 2 \times 10^{-6}$ s^{-1}),[54] aqueous solutions of organic peroxides ($J \sim 4 \times 10^{-5}$ s^{-1}),[55] organic nitrates ($J \sim 1 \times 10^{-6}$–4×10^{-5} s^{-1})[44] under clear-sky conditions. Likewise, assuming a near diffusion-limited rate for aqueous OH reaction ($k \sim 1 \times 10^{9}$ M^{-1} s^{-1})[56] and using the measured [OH] observed in California's Central Valley fog droplets ([OH] $\sim (2 \times 10^{-16}$–4×10^{-15} M),[57] a first-order rate constant range of $k_{eff} \sim (2 \times 10^{-7}$ –$4 \times 10^{-6})$ s^{-1} can be estimated for the non-selective aqueous OH reaction, which is comparable with expected J values for direct photolytic processes. Much higher [OH] values have been modeled in clouds ($\sim 10^{-13}$ M),[58,59] which would significantly increase k_{eff} relative to J. Although the importance of direct photolysis is dependent on specific atmospheric conditions and chemical system, it is expected to be the dominant photoprocessing mechanism of OM under many atmospherically-relevant scenarios.

This work focuses on the characterization of molecules produced and decomposed in the direct photolysis of aqueous extracts of SOA generated from the high-NO_x photooxidation of isoprene (C_5H_8), the most abundant non-methane hydrocarbon in the atmosphere.[60,61] We also report the effects of hydrolysis in the dark for the same SOA mixture, as this process cannot be completely decoupled from aqueous photolysis. The gas-phase photooxidation of isoprene under high-NO_x conditions produces water-soluble compounds such as organic acids, carbonyls and alcohols in the aerosol phase.[62–67] In particular, the substantial fraction of organic nitrates in the SOA (18–30% by count)[68] is expected to be photolabile, and this work is the first account of the aqueous photolysis of organic nitrates in the presence of other dissolved organic compounds. A dramatic change in the composition of aqueous isoprene SOA extracts is observed, compared to the minor change induced by hydrolysis of the same sample in the dark. The most significant change in composition is due to nitrogen-containing organic compounds (NOC), reflected by the large increase of heterocyclic compounds containing 2 nitrogen atoms.

2. Experimental

2.1. Secondary organic aerosol generation

SOA was generated from the photooxidation of isoprene in a 5 m^3 Teflon chamber and the reaction was monitored as previously described.[67,68] No inorganic seed aerosols were used. The reaction was carried out at 22 °C in the relative humidity (RH) range of 60–70%. Initial mixing ratios of isoprene (Aldrich, purity 99%), nitric oxide (NO, 5000 ppm in N_2), nitrogen dioxide (NO_2), and ozone (O_3) in the chamber were 500 ppb, 700 ppb, 100 ppb and <5 ppb, respectively. No additional precursors for the hydroxyl (OH) radicals were added. The photooxidation time was approximately 5 h. The majority of isoprene and first-generation products reacted with OH; the estimated contribution of O_3-oxidation to product formation was $<10\%$ (Fig. S1 of the ESI†). Particle mass accumulated quickly after 2 h of irradiation and SOA mass concentration reached 100 μg m^{-3} at the time of collection (Fig. S2a, ESI†). The time-dependent mixing ratios of NO, NO_y–NO, and O_3 and relevant volatile organic compounds are shown in Fig. S2a and S2b (ESI†), respectively, for a typical experiment. The SOA was collected through an activated charcoal denuder onto Teflon filters (Millipore 0.2 μm pore), which were immediately vacuum sealed and deep-frozen for offline photolysis experiments and HR-MS analysis.

2.2. Aqueous photolysis and control experiments

Filter SOA samples were extracted in 1.5–2 mL water (Fluka, HPLC grade) with 10 min sonication, used to obtain a total aqueous concentration of approximately 200 μg mL^{-1}, comparable to the high OM ratios detected in fog water.[35] Two photolysis experiments and one dark (no irradiation) control experiment were performed with the aqueous SOA extracts in otherwise identical fashion.

The light source used for photolysis experiments was a Xe arc lamp (Newport Optics model 66905 lamp housing and model 69911 power supply). A 90-degree dichroic mirror (280–500 nm) was used to reduce the visible and IR radiation, and a glass filter was used to remove UV radiation with $\lambda < 290$ nm. The wavelength dependence of the photon flux

Published on 17 May 2012 on http://pubs.rsc.org | doi:10.1039/C2CP40944E
Downloaded by PNNL Technical Library on 25 June 2012

was measured by a fiber-optic spectrometer (Ocean Optics, USB4000) and the integrated light intensity was measured by a laser power meter (Coherent FieldMate). The wavelength-dependent photon flux is shown in Fig. S3a of the ESI†, where it is compared with a modeled ground-level solar flux[69] assuming zenith angle = 0°. The main difference between the experimental flux and solar flux exists in the more-energetic $\lambda < 350$ nm region. Based on the total integrated flux for $\lambda < 350$ nm, we estimate that 1 h photolysis under our lamp equates up to 3 h photolysis under the overhead sun. The exposure durations reported in this work have not been converted to the equivalent atmospheric values.

The temperature of a blank aqueous sample was monitored under actual photolysis conditions with a K-type thermocouple (accuracy ±0.5 °C) to gauge the contribution of thermal decomposition of the sample on the time scale of the experiment. Fig. S3b of the ESI† shows that temperature in an aqueous sample increased by approximately 5 °C after 2 h and stabilized at 31 °C from 2 h to 4 h. We observe a consistent production of photoproducts throughout photolysis, which serves as an indirect indication that temperature effects were minimal. As the samples were open to air during photolysis dissolved oxygen was present in the solution, likely at the near-equilibrium solubility level.

During photolysis experiments, approximately 50 μL aliquots of the aqueous SOA sample were removed with a gas-tight syringe (Hamilton, 250 μL), without interruption of photolysis, at 0, 1, 2, and 4 h intervals for high-resolution electrospray ionization (ESI) mass spectrometry analysis. Control samples kept in the dark were analyzed similarly.

2.3. High resolution electrospray ionization mass spectrometry (HR ESI-MS)

ESI-MS experiments were performed with a high-resolution (60 000 $m/\Delta m$) linear-ion-trap (LTQ) Orbitrap™ mass spectrometer (Thermo Corp.) in the positive ion mode with a mass range of 100–2000 Da. Aqueous extracts of photolyzed SOA were directly sprayed into the mass spectrometer at a flow rate of 0.5–1 μL min^{-1} and ionized with an operating voltage of 4 kV. No other solvents were added in order to characterize only the water-soluble fraction. Analyte compounds were detected as sodiated $[M + Na]^+$ and/or protonated $[M + H]^+$ species. The instrument was calibrated with a commercial standard mixture of caffeine, MRFA, and Ultramark 1621 (LTQ ESI Positive Ion Calibration Solution, Thermo Scientific, Inc.) twice daily to maintain high mass accuracy (*ca.* 0.5 ppm at m/z 500).

Data analysis was performed similarly to our previous works.[67,68,70] A mass accuracy of better than ±0.001 Da was obtained in the m/z range of 100–1000 Da through calibration. The high mass accuracy combined with filters based on ^{13}C isotopic abundance and parity restraints[30,71] were used to unambiguously assign observed ions, whose masses generally did not exceed m/z 600. Background signals obtained from analyses of blank filters sonicated in water were deleted from sample mass spectra. Peaks in the samples that could not be unambiguously assigned to protonated or sodiated molecules with the atomic restrictions used in this work ($C_cH_hO_oN_{0-2}Na_{0-1}^+$ ions) were insignificant and accounted for *ca.* 2% of the total signal. The unassigned peaks are shown in Fig. S4 (ESI†). Mass spectra shown henceforth present only assigned peaks, with the m/z values converted into the molecular weights of the corresponding neutral precursors.

The signal intensities of the detected molecules were converted to approximate mass concentration using an ESI sensitivity calibration approach described elsewhere.[72] The calibration was performed with multifunctional carboxylic acid standards, followed by scaling the summed signal by the total organic mass concentration (~200 μg mL^{-1}). It is important to emphasize that due to the simplifying assumptions made in the sensitivity calibration, the analyte concentrations should be treated as an *approximation* and any errors are reported as a measure of precision (one standard deviation of duplicate trials) not as estimates of accuracy. Fig. S4 (ESI†) shows raw intensity distributions for SOA mass spectra, which are not drastically altered by the intensity-to-mass conversion. Data in the text will be henceforth presented in terms of mass concentration in units of μg mL^{-1}.

2.4. Multistage tandem mass spectrometry (MS^n)

Multistage tandem mass spectrometry (MS^n, $n = 2, 3$) experiments were performed for ions of interest by mass isolation followed by collision induced dissociation (CID) in the linear ion trap. This analysis was repeated at the MS^3 level for product ions obtained in the MS^2 stage if there was sufficient signal. Ions subjected to CID eliminate neutral fragments, which in some cases can be used to characterize the structure of the molecules. The collision energy was adjusted so that the precursor ion peak was retained in the MS^n spectra at relative intensities > 10%. The product ions were analyzed in the high-resolution Orbitrap mass analyzer where they could be unambiguously identified. MS^n analyses were performed for product or degraded peaks of interest in photolyzed SOA samples (preliminary experiments were done to obtain m/z positions of product and degraded peaks). MS^n also confirmed that compounds examined in this work are covalently bonded (determined by threshold CID energy needed to fragment covalent ions *vs.* dimers and complexes of standard compounds listed in Table S1, ESI†).

2.5. Ion chromatography

Ion chromatography (IC, Metrohm Inc.) analyses were performed using a thermal conductivity detector on the control and photolyzed samples in both the positive and negative ion modes to quantify the amounts of nitrates, nitrites, and other inorganic ion impurities. In the positive ion mode, calibration was performed in the 0.25–10 ppm range for the following ions: Li^+, Na^+, NH_4^+, K^+, Ca^{2+} and Mg^{2+} on a commercial cation column (Metrosep C4 - 250/4.0). Positive ion mode measurements did not determine significant concentrations of cations. In the negative ion mode, calibration was performed in the 0.33–10 ppm range for the following ions: F^-, Cl^-, NO_2^-, Br^-, NO_3^-, PO_4^{3-} and SO_4^{2-} on a commercial anion column with chemical suppression (Metrosep A Supp 5 150/4 mm). Ionic peaks were not observed in pure water blanks. Peaks were well-resolved and calibration fits were

 This journal is © the Owner Societies 2012

Published on 17 May 2012 on http://pubs.rsc.org | doi:10.1039/C2CP40944E
Downloaded by PNNL Technical Library on 25 June 2012

linear for all ions with R^2 values >0.999. Section S1 in the ESI† describes measurements of aqueous precursors for the OH radical in further detail, including NO_2^- and NO_3^- that are measured by IC, and ROOH that is measured by a colorimetric test.[73] We estimate based on known radical yields that less than 1% of the changes in composition are due to OH chemistry competing with direct photolysis.

3. Results and discussion

3.1. Photolysis induced changes in composition

Fig. 1 shows representative mass spectra of SOA samples during photolysis and control experiments for the 0 h and 4 h reaction time (1 h and 2 h mass spectra are omitted from Fig. 1). The mass spectra change significantly upon photolytic processing. Notably, the higher-MW (400–500 Da) compounds are efficiently converted to lower-MW compounds (150–250 Da) with an accompanying shift in the distribution of mass concentrations. In contrast, hydrolysis does not significantly change the mass spectra. For example, the concentration of the most abundant compound in aqueous isoprene SOA, $C_{10}H_{16}O_8$, detected as a sodiated peak at m/z 287.0738, remains constant within 4 h in the dark (47 ± 2 μg mL^{-1}) but decreases to ~36 μg mL^{-1} after 4 h of photolysis. The MS^n analysis of $C_{10}H_{16}O_8$ suggests that this molecule is formed by condensation of two 2-methylglyceric acid (2MGA, $C_4H_8O_4$) units with $C_2H_4O_2$.

We estimate that no more than 35%, by count, of the peaks in the initial SOA mass spectrum are retained following 4 h photolysis, and 65% of the initially-observed peaks are replaced by photoproduct peaks. It is not straightforward to discern if the initially present peaks that remain in the mass spectra are inert with respect to photolysis because the corresponding compounds may be both formed and decomposed by photolysis. Furthermore, some peaks may represent multiple isomeric compounds, some of which are photolabile while the others are not. The majority of the peaks that remain also

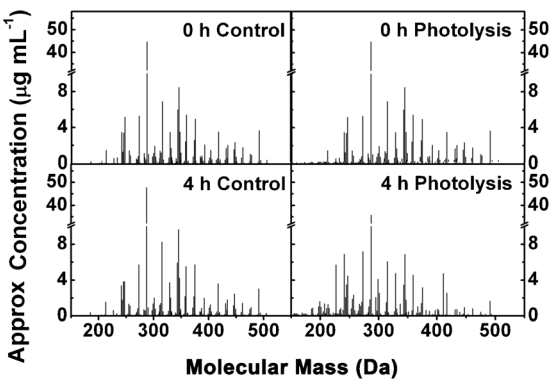

Fig. 1 Mass spectra of the aqueous SOA extract detected in ESI positive ion mode and converted to neutral molecular formulas for the dark control (panels on the left) and photolysis (panels on the right) experiments for 0 h and 4 h time intervals. Peaks are normalized with respect to the total mass concentration (200 μg mL^{-1}) in the sample. The most abundantly observed compound is sodiated $C_{10}H_{16}O_8$. Mass spectra are also plotted with respect to normalized signal-to-noise in the ESI†, Fig. S4. Note the breaks in the vertical axis.

change in concentration, *e.g.*, 30% of peaks retained in the 4 h sample have increased or decreased in concentration by more than a factor of 2. In comparison, 73% of the total number of peaks was conserved in the control spectra after 4 hours in the dark.

The control experiments demonstrate that a non-negligible number of compounds in isoprene SOA photooxidation may hydrolyze to some extent at room temperature. We discuss photolysis-induced changes henceforth in this work with respect to changes induced by hydrolysis, which we would refer as "control samples" in figures and discussion. Changes in mass concentration (ρ, μg mL^{-1}) were calculated using eqn (1) separately for photoproducts and photodegraded compounds in the 4 h compared to the 0 h samples for the control and photolysis experiments. (In this work, we define "photoproduct" and "photodegraded" compounds as those with ion abundances that *steadily* increase ($\Delta\rho/\Delta t > 0$) or decrease ($\Delta\rho/\Delta t < 0$), respectively, during the *entire* reaction timescale).

$$\text{Change} = 100\%[\Sigma\rho_{4h} - \Sigma\rho_{0h}]_{\text{produced or degraded}}/200\ \mu\text{g mL}^{-1} \quad \text{(E1)}$$

The changes in mass concentration induced by hydrolysis are significantly smaller (±1–2%) compared to photolysis (~±29–32%) within a 4 h time period.

The average elemental ratios (H/C, O/C, and N/C), average molecular size (parameterized by the number of C atoms per molecule), and number of N atoms in the molecule, and aromaticity index (AI)[74] are extracted from the assigned molecular formulas. For brevity, we denote compounds $C_cH_hO_oN_n$ where $n = (0, 1, 2)$ as 0N, 1N, and 2N compounds, respectively. These averaged quantities can be used to evaluate the overall change in the SOA composition. All averaged quantities are calculated with respect to ρ for *all* observed compounds as shown below (note: calculations weighted by raw peak intensities yielded similar results):

$$\langle X/C\rangle = \Sigma(X\rho)/\Sigma(C\rho) \quad (X = O, H, N) \quad \text{(E2)}$$

$$\langle C\rangle = \Sigma C\rho/\Sigma\rho \quad \text{(E3)}$$

$$\%\ n\text{N compounds} = 100\%(\Sigma\rho_{n\text{N}}/\Sigma\rho) \quad (n = 0, 1, 2) \quad \text{(E4)}$$

$$\text{AI} = (1 + c - o - 0.5h)/(c - o - n) \quad \text{(E5)}$$

$$\%\ \text{Aromaticity} = 100\%(\Sigma\rho_{\text{AI}>0.67}/\Sigma\rho) \quad \text{(E6)}$$

For $C_cH_hO_oN_n$ compounds, eqn (5) defines AI as the total number of double bonds that do not include heteroatoms. Therefore, AI > 0 correlates to a positive number of carbon–carbon double bonds and AI > 0.67 (E6) suggests condensed aromatic structures in a molecule.[74] The results from the statistical analyses of photolysis and control samples are compiled in Table 1 for each reaction time interval. Fig. 2 shows the time-dependent changes in the averaged number of carbon atoms ⟨C⟩ of all the SOA compounds, and ratios of ⟨O/C⟩, ⟨H/C⟩, ⟨N/C⟩. Fig. 3 shows the mass % of 0N, 1N and 2N compounds, and % of aromatic compounds in the photolysis and dark control samples. Negligible changes in average

Published on 17 May 2012 on http://pubs.rsc.org | doi:10.1039/C2CP40944E
Downloaded by PNNL Technical Library on 25 June 2012

Table 1 Average mass-weighted number of carbon atoms, elemental ratios, and percent abundance of molecules with high aromaticity index (AI > 0.67), 0N ($C_cH_hO_o$), 1N ($C_cH_hO_oN$), and 2N ($C_cH_hO_oN_2$) compounds at various photolysis and dark reaction times. Errors are reported as 1σ spread between experiments, where applicable

Photolysis	⟨C⟩	⟨O/C⟩	⟨H/C⟩	⟨N/C⟩	% Arom.	% 0N	% 1N	% 2N
0 h	12.1	0.771	1.553	0.007	3.7	92.8	6.2	1.1
	(0.0)	(0.008)	(0.001)	(0.001)	(0.9)	(0.6)	(0.4)	(0.9)
1 h	10.8	0.792	1.549	0.020	10.1	88.4	2.6	9.0
	(0.6)	(0.001)	(0.012)	(0.009)	(3.7)	(4.1)	(0.2)	(4.3)
2 h	10.5	0.793	1.545	0.028	13.7	84.1	3.3	12.6
	(0.5)	(0.000)	(0.013)	(0.014)	(5.9)	(7.1)	(0.9)	(6.2)
4 h	10.3	0.807	1.526	0.039	19.4	78.8	2.3	18.9
	(0.4)	(0.000)	(0.010)	(0.011)	(4.2)	(4.9)	(0.4)	(4.4)
Control	⟨C⟩	⟨O/C⟩	⟨H/C⟩	⟨N/C⟩	% Arom.	% 0N	% 1N	% 2N
0 h	12.1	0.779	1.551	0.006	2.6	93.3	6.6	0.1
1 h	11.9	0.788	1.549	0.005	2.7	93.8	6.1	0.1
2 h	12.0	0.785	1.551	0.005	2.9	94.0	5.8	0.1
4 h	11.9	0.787	1.550	0.005	2.5	94.7	5.2	0.1

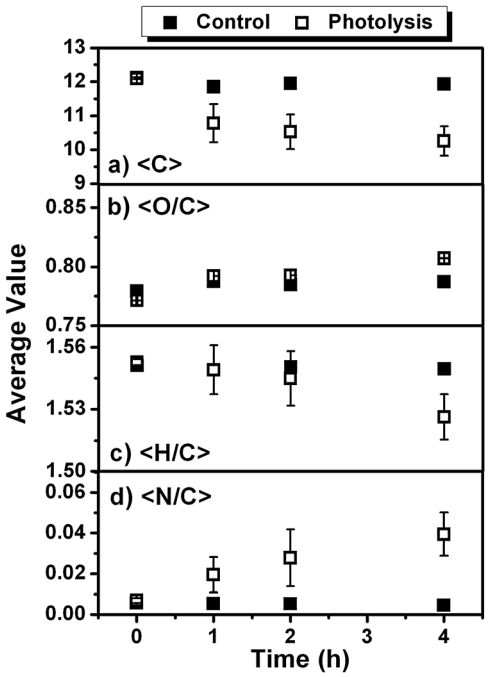

Fig. 2 Changes in the average (a) number of carbon atoms and (b–d) elemental ratios of compounds in the photolysis and dark control samples with respect to time of photolysis (open markers) or hydrolysis (closed markers). Errors represent 1σ between repeated experiments.

quantities were observed in the control samples, with the exception of 1N compounds that decreased slowly in the dark.

Fig. 2a shows that initially the SOA compounds have an average of 12 carbons in their molecular structure. After 4 h of photolysis, ⟨C⟩ is reduced to approximately 10 carbons. The trend in ⟨C⟩ mirrors the observation that high-MW oligomers are degraded, as reflected in the evolution of the mass spectra shown in Fig. 1. Degradation of oligomer peaks was also an important result in the aqueous direct photolysis of limonene ozonolysis SOA.[54] In contrast, indirect photolysis studies of model organic compounds typically form high-MW compounds instead of degrading them.[15]

The ⟨O/C⟩ traditionally describes the degree of oxidation of a compound. In isoprene SOA, ⟨O/C⟩ for the water-soluble fraction is ~0.77 and increases slightly to ~0.81 following 4 h of photolysis (Fig. 2b). The results from our work are in good agreement with the observations by Bateman *et al.* (2011). The net increase in ⟨O/C⟩ may be due to the production of high-O/C molecules as a result of photodegradation of low-O/C molecules in water, as proposed by Bateman *et al.* (2011). This explanation is qualitatively consistent with aqueous photolysis studies of natural organic matter.[75,76] In our experiments, the increase in the ⟨O/C⟩ in photolyzed SOA samples cannot be attributed to aqueous OH-oxidation chemistry because OH formation is not expected to be significant (Section S1, ESI†).

The ⟨H/C⟩ is a good indicator of the degree of unsaturation in SOA molecules. Our data show that ⟨H/C⟩ is decreasing (ΔH/C ~ −0.03 in 4 h) with respect to photolysis time (Fig. 2c). The decrease in H/C in the SOA compounds for our samples can be attributed to the photoformation of molecules with double bonds or rings. Our observations are different from those of Bateman *et al.* (2011), who reported the opposite trend for the limonene/O_3 SOA system. The ozonolysis system may behave differently than the high-NO_x photooxidation SOA studied in this work. The high concentration (10^{-5} M) peroxide quantified in the work of Bateman *et al.* (2011) may produce OH radicals upon photolysis to destroy intact C=C bonds left over from the incomplete oxidation of limonene. In our experiments, we expect a relatively complete oxidation of double bonds from of isoprene and its first-generation products (Fig. S2, ESI†) prior to SOA collection and we quantified the concentrations of OH precursors (Section S1, ESI†) in this work to be negligible.

The ⟨N/C⟩ has been quantified in lab-generated[70] and ambient[77] biogenic OA samples in the range of 0.02–0.03. Urban OA may have ⟨N/C⟩ in the range of 0.01–0.09.[78–81] This work determines ⟨N/C⟩ of the water-soluble fraction of isoprene photooxidation SOA to be ~0.01, a value that increases to ~0.04 after 4 h of photolysis (Fig. 2c). The increase in N/C ratio suggests that the nitrogen mass is not conserved and we speculate that the poorly-ionizable organic nitrates present only in the background may be transformed into more highly-ionizable nitrogen products. Considering the small initial ⟨N/C⟩ observed in aerosol samples, the fourfold increase in ⟨N/C⟩ during 4 h photolysis is substantial.

Effect of photolysis on the distribution of N atoms in the molecules is similarly dramatic. The mass fraction of water-soluble 0N compounds is dominant (93%) initially in the high-NO_x isoprene SOA. This fraction increases slightly (to 95%) after 4 h in the dark as organic nitrates are hydrolyzed to alcohols.[9,82] However, photolysis degrades 0N compounds (Fig. 3a) and reduces the 0N fraction to an average of 79% after 4 h. This net loss in 0N compounds occurs despite simultaneous production of different 0N compounds in the photoproduct pool (Section 3.5). A net loss is also observed for 1N compounds, which are known to be organic nitrates[62,65,68,83] and further verified by MS^n in this work. The 1N compounds are present at ~6% initial fraction and are reduced to ~5% from 4 h hydrolysis in the dark.

This journal is © the Owner Societies 2012

Published on 17 May 2012 on http://pubs.rsc.org | doi:10.1039/C2CP40944E
Downloaded by PNNL Technical Library on 25 June 2012

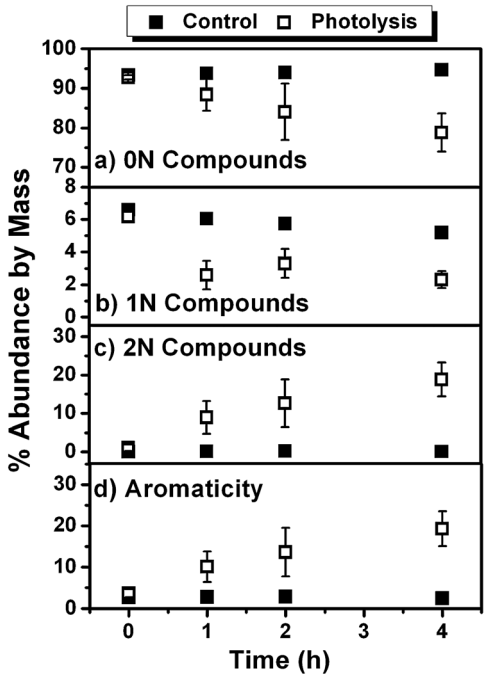

Fig. 3 Changes in mass abundance of compounds with (a) 0N ($C_xH_yO_z$), (b) 1N ($C_xH_yO_zN$), (c) 2N ($C_xH_yO_zN_2$) and (d) compounds with high aromaticity index (AI > 0.67) in the photolysis (open markers) and dark control (closed markers) samples with respect to time. Errors represent 1σ between repeated experiments.

The effect of hydrolysis on 1N compounds is clear from the slow linear decline in the concentration of 1N compounds (Fig. 3c). However, photolysis is a faster loss mechanism for these organic nitrates. After 4 h photolysis the fraction of 1N compounds is reduced to ~2%, a four-fold enhancement in the loss rate compared to hydrolysis. We note that nitrates may be underrepresented in our work due to their low ionization efficiencies in the positive ion mode, so the effect of photolysis may in fact be greater.

A large increase in 2N compounds is observed after 4 h photolysis (Fig. 3c), which increases the N/C of the sample mixture despite photolysis of organic nitrates. Before irradiation, 2N compounds, most likely dinitrates,[65] comprise less than 1% of the SOA molecular pool, a result consistent with our earlier work.[68] The fraction of 2N compounds increases up to 19% after 4 h photolysis. This large increase in 2N compounds is unexpected as such a substantial change in the distribution of NOC during photolysis of dissolved organic material has not been previously observed.

The differences in the mass fractions do not appear to add up: 1N fraction is reduced from 6% to 2% whereas 2N fraction is increased from 1% to 19%. We partially attribute this inconsistency to a change in the ionization efficiencies between the 1N precursors and 2N photoproducts. For example, the proton affinity of a 2N heterocyclic NOC may be greater than a 1N alkyl nitrate of comparable molecular size by >200 kJ mol^{-1}.[84] Additionally a portion of the 2N products may be produced from the inorganic nitrogen initially present (presumably from nitric acid and HONO in the chamber). The already poor ionization efficiencies for these organic nitrates (the majority of the 1N compounds) are further reduced if they have low-MW and if the ionization happens in water. It's possible that the photolysis of non-ionizable 1N compounds (that are undetected) serves as a partial source of nitrogen to produce larger and more easily ionizable 2N compounds. Furthermore, our results from MS^n (Section 3.5) show that the fragmentation signatures of these 2N compounds are not consistent with organic dinitrates. Instead, the 2N photoproducts may be the type of nitrogen compounds that have high efficiency in ESI, *e.g.* heterocyclic nitrogen. Therefore, the mass fraction of 1N and 2N compounds should be considered lower and upper limits, respectively.

The increase in the degree of unsaturation, ⟨N/C⟩ and % of 2N compounds is reflected in the increase in abundance of possibly-aromatic molecules (those with AI > 0.67) (Fig. 3d). The fraction of possibly aromatic SOA compounds is ~4% initially and increases to ~20% after 4 h of photolysis. The large increase in AI is consistent with both the photoproduction of alkenyl moieties from Norrish II photochemistry of larger (> C_4) carbonyls[85] and the production of aromatic 2N species. Table 1 shows that the mass percent of 2N compounds and those with AI > 0.67 are roughly equivalent throughout the photolysis experiment, suggesting that the 2N products or their precursors are aromatic species.

3.2. Specific photodegraded compounds

The main advantage of HR-MS is its ability to simultaneously detect a large number of individual compounds. There were approximately 50 specific compounds (out of *ca.* 300 observed) in each sample whose mass concentration decreased consistently over photolysis period. The identities and mass concentrations of the photodegraded compounds reproducibly observed between duplicate trials are shown in Table 2, and the entire list of compounds whose concentration steadily decreased due to photolysis or dark hydrolysis (control) is shown in Table S2a and S2b of the ESI†. The photodegraded compounds can be quite large, up to 18 carbons in length. Table 2 shows that 0N and 1N compounds are predominantly photodegraded, consistent with the expectation that carbonyls and nitrates in isoprene SOA are readily photolyzed. The formulas of NOCs listed in Table 1 correspond to ester oligomers of 2MGA and its nitrate derivatives (2MGAN, $C_4H_7O_6N$). These nitrate esters of 2MGA have been previously characterized in isoprene SOA by us[70] and other groups.[62,83] For example, it has been demonstrated that $C_8H_{13}O_9N$ is formed through condensation of 2MGA and 2MGAN, and $C_{12}H_{19}O_{12}N$ is a product of condensation of two 2MGA units and one 2MGAN unit.

Table 3a shows average characteristics for compounds degraded by photolysis. For example, photodegraded molecules are larger than the average SOA compound, *e.g.* ⟨C⟩ = 14 for the photodegraded compounds compared to a smaller value of ⟨C⟩ = 12 for the entire SOA sample. In general the elemental ratios for the degraded compounds are similar to that for the SOA. Separating the degraded compounds into NOC and non-NOC fractions can be instructive. The NOC fraction has a much higher ⟨O/C⟩, again consistent with NOC being oxygen-rich organic nitrates bearing three O atoms in

Published on 17 May 2012 on http://pubs.rsc.org | doi:10.1039/C2CP40944E
Downloaded by PNNL Technical Library on 25 June 2012

Table 2 List of compounds reproducibly degraded from irradiation of aqueous isoprene high-NO_x SOA samples. The rates of degradation are derived from linear fits of concentration *vs.* time profiles. Errors in the initial concentration of a compound in the SOA extract are reported as 1σ spread between experiments, and errors in the rate of decrease due to photolysis are reported as deviations in the slope. Compounds are sorted by increasing number of carbon atoms

Molecular formula	Concentration in SOA (μg mL^{-1})	Rate of change (μg mL^{-1} h^{-1})
$C_8H_{13}O_9N$[a,b,c]	0.88 (±0.11)	−0.17 (±0.06)
$C_{12}H_{19}O_{12}N$[a,b,c]	1.70 (±0.35)	−0.35 (±0.17)
$C_{12}H_{20}O_{10}$	2.65 (±0.82)	−0.38 (±0.15)
$C_{13}H_{19}O_{11}N$	0.26 (±0.02)	−0.06 (±0.03)
$C_{13}H_{22}O_9$	0.11 (±0.01)	−0.03 (±0.01)
$C_{14}H_{20}O_9$	0.27 (±0.05)	−0.05 (±0.01)
$C_{14}H_{21}O_{13}N$[a]	2.20 (±0.19)	−0.39 (±0.21)
$C_{14}H_{22}O_{10}$	2.93 (±0.38)	−0.46 (±0.19)
$C_{14}H_{22}O_{11}$	23.33 (±1.66)	−3.23 (±1.60)
$C_{14}H_{24}O_8$	0.28 (±0.15)	−0.05 (±0.02)
$C_{15}H_{22}O_{12}$	3.33 (±0.16)	−0.43 (±0.29)
$C_{15}H_{24}O_9$	0.53 (±0.08)	−0.12 (±0.05)
$C_{16}H_{24}O_{11}$	0.50 (±0.02)	−0.08 (±0.04)
$C_{16}H_{24}O_{12}$	1.83 (±0.17)	−0.30 (±0.12)
$C_{17}H_{26}O_{11}$	0.32 (±0.02)	−0.07 (±0.03)
$C_{17}H_{26}O_{13}$	1.84 (±0.10)	−0.32 (±0.14)
$C_{18}H_{28}O_{14}$	3.48 (±0.16)	−0.66 (±0.45)

Structures previously reported by: [a] Ref. 68. [b] Ref. 62. [c] Ref. 83.

Table 3 Average number of carbon atoms and elemental ratios for all formed and degraded peaks, segregated into NOC (1N and 2N) and non-NOC (0N) fractions

	⟨C⟩	⟨H/C⟩	⟨O/C⟩	⟨N/C⟩
(a) Degraded compounds				
Total	14	1.54	0.79	0.01
Non-NOC fraction	14	1.54	0.77	0.00
NOC fraction	13	1.67	0.93	0.05
(b) Product compounds				
Total	9	1.45	0.88	0.10
Non-NOC fraction	10	1.54	0.68	0.00
NOC fraction	8	1.32	1.17	0.25

nitrate groups. The ⟨H/C⟩ is also higher in the NOC fraction because the formation of organic nitrates does not involve H abstraction by molecular oxygen like in the formation of carbonyls from alkoxy radicals.

The time-dependent concentrations of two select 1N and two select 0N compounds are shown in Fig. 4a, b and 5c, d, respectively. The mass concentration changes significantly due to photolysis for these molecules; for example, the aforementioned 2MGA–2MGAN dimer ($C_8H_{13}O_9N$) remains at roughly 1 μg mL^{-1} in solution if kept in the dark but is almost completely degraded at the end of the 4 h photolysis experiment. Fig. 3b suggests that some 1N compounds may hydrolyze more quickly than $C_8H_{13}O_9N$ and Table S2b (ESI†) lists several examples of 1N compounds susceptible to hydrolysis. NOC that are able to hydrolyze may be tertiary nitrates.[9] Our data indicate that the non-hydrolyzable organic nitrates are the major fraction of NOC in isoprene SOA, and that photolysis is a faster route to the decomposition of all NOC present in isoprene SOA compared to hydrolysis, regardless of their specific structure.

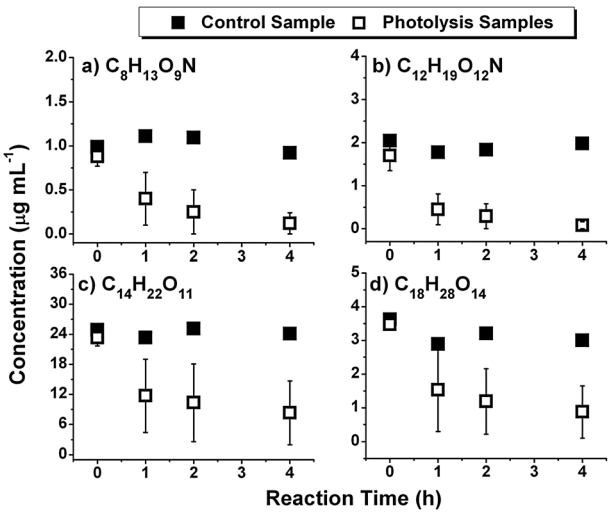

Fig. 4 Time-dependent abundance for select peaks degraded in the photolysis samples. The same peaks do not decrease in abundance with the same rate in the control samples. Errors represent 1σ between repeated experiments.

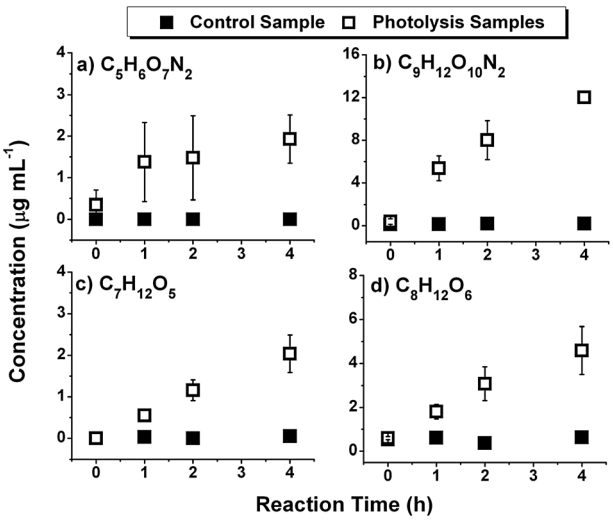

Fig. 5 Time-dependent abundance for select peaks produced in the photolysis samples. The same peaks do not increase in abundance in the control samples. Errors represent 1σ between repeated experiments.

3.3. Specific photoproducts

There were approximately 40 specific compounds in each sample whose mass concentration increased consistently over the photolysis period. In comparison, there were only 5 compounds in the dark control sample that increased in concentration and they are likely hydrolysis products. The photoproducts that were reproducibly observed between photolysis trials are reported in Table 4. The full list of photoproducts and hydrolysis products is available in Table S3a and S3b (ESI†). The photoproducts shown in Table 4 are comprised of 0N and 2N compounds with generally zero or small initial concentrations. There are some exceptions of compounds, such as $C_{11}H_{16}O_8$ and $C_8H_{12}O_6$, which are already present at substantial initial concentrations in the SOA. It is likely that the photolysis of higher-MW oligomer

 This journal is © the Owner Societies 2012

View Online

Published on 17 May 2012 on http://pubs.rsc.org | doi:10.1039/C2CP40944E
Downloaded by PNNL Technical Library on 25 June 2012

Table 4 List of compounds reproducibly formed by irradiation of aqueous isoprene high-NO_x SOA samples. The rates of formation are derived from linear fits of concentration *vs.* time profiles. Errors in the initial concentration of a compound in the SOA extract are reported as 1σ between trials and errors in the rate of increase due to photolysis are reported as deviations from a linear slope. Compounds are sorted by increasing number of carbon atoms

Molecular formula	Concentration in SOA ($\mu g\ mL^{-1}$)	Rate of change ($\mu g\ mL^{-1}\ h^{-1}$)
$C_5H_6O_7N_2$	0.35 (±0.35)	0.35 (±0.12)
$C_5H_{12}O_4$	0.00 (±0.00)	0.07 (±0.01)
$C_6H_6O_8N_2$	0.17 (±0.17)	0.29 (±0.06)
$C_7H_8O_9N_2$	0.09 (±0.09)	0.26 (±0.06)
$C_7H_{10}O_9N_2$	0.30 (±0.30)	1.24 (±0.20)
$C_7H_{12}O_5$	0.00 (±0.00)	0.51 (±0.03)
$C_7H_{12}O_6$	0.00 (±0.00)	0.13 (±0.02)
$C_8H_{10}O_8N_2$	0.16 (±0.16)	0.32 (±0.13)
$C_8H_{10}O_{10}N_2$	0.42 (±0.11)	1.29 (±0.24)
$C_8H_{12}O_4$	0.00 (±0.00)	0.06 (±0.01)
$C_8H_{12}O_6$	0.60 (±0.07)	0.99 (±0.09)
$C_9H_{12}O_{10}N_2$	0.39 (±0.26)	2.78 (±0.46)
$C_{10}H_{16}O_5$	0.24 (±0.18)	0.18 (±0.03)
$C_{11}H_{16}O_6$	0.16 (±0.11)	0.10 (±0.03)
$C_{11}H_{16}O_8$	1.23 (±0.15)	1.07 (±0.06)

species generates monomeric compounds that are already present in the original SOA extract.

Fig. 5 shows the changes in mass concentration with respect to photolysis time for select 2N (Fig. 5a and b) and 0N (Fig. 5c and d) products. These compounds are not produced in the absence of irradiation. Many of the photoproducts increase with time linearly during the 4 h of photolysis. However, some species show a saturation behavior that may be attributed to the complete consumption of precursor molecule(s) or their own photodegradation. The apparent concentrations of some NOC products are high ($>10\ \mu g\ mL^{-1}$ out of $200\ \mu g\ mL^{-1}$ total organics) at the end of 4 h. However, as previously discussed, these nitrogen compounds may be overrepresented in ESI techniques, and the mass concentration of photoproduct NOC should be treated as an upper limit.

The steady growth of 2N photoproducts is an important, and non-obvious, result. As studies of direct photolysis of complex mixtures comprising organic nitrates and oxygenated compounds are not available in the literature, the observations in this work cannot be compared to others. The particular 2N products shown in Table 4 are generally small ($<C_8$) and highly oxidized. Table 3b shows average characteristics for only photoproducts, which are smaller ($\langle C\rangle = 9$) than non-photolyzed SOA compounds ($\langle C\rangle = 12$). The $\langle O/C\rangle$ and $\langle N/C\rangle$ for photoproducts are higher than the average for the SOA, and the H/C ratio is lower, which are expected results based on Fig. 2b. Again, we can separate the photoproducts into NOC and non-NOC fractions. The non-NOC fraction is larger by 1 carbon and has a lower $\langle O/C\rangle$ (0.68) and higher $\langle H/C\rangle$ (1.54) than the corresponding values for all the photoproducts. We can speculate that the lower $\langle O/C\rangle$ of the non-NOC compounds may be due to some extent to decarboxylation of the precursor 0N compounds (loss of CO_2).

Conversely, the NOC products, *i.e.*, 2N compounds, are generally 1 carbon smaller, have smaller $\langle H/C\rangle$ (1.32) and higher $\langle O/C\rangle$ (1.17) compared to all photoproducts. The $\langle H/C\rangle$ of the 2N photoproducts are characteristic of aromatic molecules. For example, unsaturated molecules that are aromatic, *e.g.*, benzene (C_6H_6, H/C = 1.0) or trimethylbenzene (C_9H_{12}, H/C = 1.33), have much lower H/C than unsaturated molecules that are aliphatic, *e.g.*, limonene ($C_{10}H_{16}$, H/C = 1.6) or squalene ($C_{30}H_{50}$, H/C = 1.7). Furthermore, H/C values show little variability for aliphatic molecules initially present in aqueous isoprene SOA. For example, the spread in $\langle H/C\rangle$ for all observed molecular formulas is small (1.55 ± 0.14). This places the H/C value for NOC products outside the expected range (note the quoted error value is the standard deviation in all observed $\langle H/C\rangle$ in one data set and is different from the standard deviation between trials presented in Table 1) and further suggests that the 2N photoproducts are heterocyclic and/or aromatic. MS^n experiments can differentiate between nitrate and other types of nitrogen functional group and indeed results from Section 3.4 support the suggestion that 2N compounds are heterocyclic and/or aromatic. The $\langle O/C\rangle$ is also unexpectedly high for the 2N photoproducts, indicating that oxidized nitrogen species are present in the formation steps of 2N products.

3.4. MS^n characterization of degraded compounds and photoproducts

MS^n studies provide valuable insight into the chemical structure of organic molecules. Neutral loss fragments resulting from CID can be used to characterize certain classes of compounds. For example, past work on isoprene SOA determined that organic nitrates tend to lose neutral molecules of the type RNO_x (*e.g.*, HNO_3, CH_3NO_3, HNO_2, *etc.*). Furthermore the characteristic neutral loss of $C_4H_6O_3$ for 2MGA oligomers was determined using fragmentation studies[62,68] and the ester functionality was confirmed by chromatography techniques.[63] In order to better understand fragmentation patterns for the instrument conditions used in our work we first performed MS^n experiments for several organic acids listed in Table S1 (ESI†). The resulting neutral loss patterns of standards are compiled in the same table. Losses of CO, H_2O, and C_2H_2O were observed for aliphatic acids, and CO_2 loss was observed for the singular aromatic acid used in the study. None of the standard acid monomers or dimers lost $C_4H_6O_3$, confirming that loss of $C_4H_6O_3$ is characteristic of 2MGA oligomers when considering isoprene SOA and similar compounds.

Fig. 6 shows combined fragmentation results of MS^n characterization of photodegraded compounds and photoproducts observed with sufficient signal and in the absence of interfering peaks. Fragmentation was performed on more than 10 peaks in each case and the results from MS^2 and MS^3 are combined for a particular peak in order to make general comments about the chemical nature of photodegraded and photoproduct compounds. The photodegraded NOC lost neutral RNO_x fragments, in good agreement with previous reports. The photodegraded 0N compounds lost primarily $C_4H_6O_3$. A signature fragmentation pattern emerged for photolyzed 0N compounds in that the major loss is $C_4H_6O_3$ (normalized to 100%), followed by $C_8H_{12}O_6$ (4–6%), HCOOH (3–4%) and H_2O (1–3%). These results suggest that degraded compounds are chemically homogeneous. Similar to our previous work,[68]

Published on 17 May 2012 on http://pubs.rsc.org | doi:10.1039/C2CP40944E
Downloaded by PNNL Technical Library on 25 June 2012

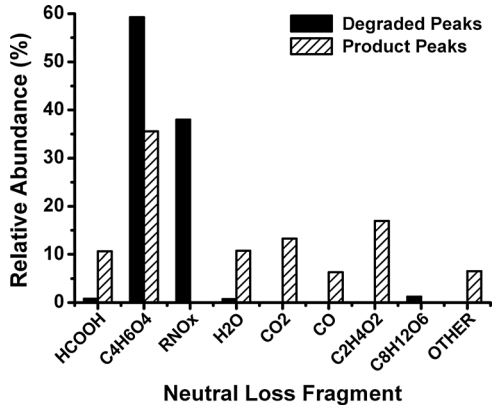

Fig. 6 Most abundant neutral losses in MS^n experiments of photodegraded and ptotoproduct peaks. RNO_x fragments (where R can be H and $x = 1, 2, 3$) correspond to the sum of neutral losses from alkyl nitrates because all N-containing neutral losses from organic nitrates conserve the N–O bond. The category of "other" losses corresponds to infrequently-observed carbon fragments like $C_4H_6O_3$.

the loss of $C_4H_6O_3$ here suggests that the compounds undergoing CID are esters of 2MGA, and the loss of HCOOH suggests that there are hydroxyl groups in alpha positions relative to carboxylic acid groups. The ester group is not known to be photolabile and is unlikely to be the part of the 2MGA oligomer that absorbs light and decomposes. Rather, these are likely carbonyl groups in the multifunctional oligomers that were photodegraded.[85] Furthermore, the MS^n experiments indicate that the ester functionality is still present in the degraded molecules.

A common fragmentation pattern was not observed for photoproducts. The various losses shown in Fig. 6 indicate that photoproducts are a diverse set of molecules, suggesting that photolysis introduces more heterogeneity in the dissolved organic composition. For example, the primary neutral loss for two photoproducts, $C_8H_{12}O_6$ and $C_{11}H_{16}O_8$, was HCOOH and $C_4H_6O_3$, respectively. The category of "other" losses shown in Fig. 6 includes a compilation of C_1–C_4 carbon fragments, *e.g.*, $C_3H_4O_3$ (pyruvic acid), which was observed only once. Losses of $C_2H_4O_2$, $C_4H_6O_3$, H_2O and CO observed for 0N photoproducts indicate that, as expected, photolysis results in formation of multifunctional acids, carbonyls or alcohols.

Unlike photodegraded compounds, 2N photoproducts do not lose RNO_x fragments. Fig. 7 shows MS^n data for a representative 2N product, $C_5H_6O_7N_2$, where the neutral losses are not consistent with nitrate ($-RNO_x$), amine ($-RNH_2$), or imine (–RNH) functional groups. Instead the smallest product ion, *e.g.* m/z 103.0138 or $C_2H_3N_2O_3^+$, still contains two nitrogen atoms. The presence of two nitrogen atoms in the most stable part of the molecule indicates that the 2N compounds are cyclic or aromatic. Certain types of heterocyclic 2N compounds with reduced nitrogen atoms, *e.g.*, imidazoles, pyrazole, pyrazines, *etc.*,[86] have been previously associated with SOA. However, this particular product has very high oxygen content, which does not correlate with reduced 2N heterocyclic core structures. Rather, the most reasonable interpretation for the product ion $C_2H_3N_2O_3^+$ is

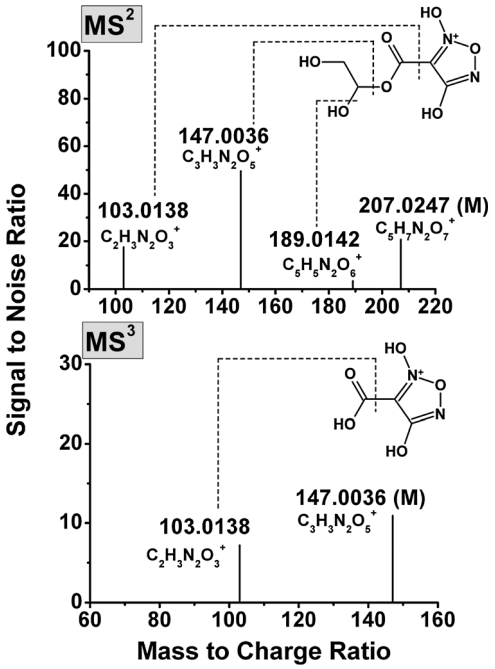

Fig. 7 MS^{2-3} spectra for protonated $C_5H_6O_7N_2$, with possible fragmentation routes leading to product ions illustrated as dashed lines at the cleavage sites (generally accompanied by H transfer). Structural characterization of the protonated photoproduct is consistent with a heterocyclic structure.

a hydroxylated furoxan structure as shown in Fig. 7. Furoxans are the N-oxide of furazan and are important biological moieties.[87] Alternatively, $C_2H_3N_2O_3^+$ may be visualized as having an N=N bond instead of two C=N bonds, and there is not sufficient information to discriminate between these different structures. The formation of furoxan-like derivatives is consistent with all of the observations derived from HR-MS and HR-MS^n. Specifically, they have sufficiently high O/C, high N/C, low H/C and are not likely to produce RNO_x neutral losses in CID. We emphasize that the probability of incorrect assignment or interference for a low-MW ion at m/z 103.0138 is very small.

Additionally, CO_2 neutral loses were prominent in the fragmentation of some 2N products. CO_2 loss is not common in the positive ion mode.[88,89] However, we observe this loss as the dominant fragmentation channel for dihydroxybenzoic acid, the only aromatic acid standard in our fragmentation study. In light of other evidence, namely low H/C of photoproducts and MS^n signatures, the CO_2 loss from our limited fragmentation experiments is consistent with aromatics being formed during photolysis. Therefore, we hypothesize that cyclization reactions of organic nitrogen oxides may be induced by photolysis to form stable 2N heterocyclic molecules and we discuss possible routes to their formation in the following section.

3.5. Mechanism of formation for NOC

The aqueous photolytic processing of the complex SOA involves a vast number of radical combination reactions resulting in formation of photostable products. The majority of photoproducts by count observed in this work do not

 This journal is © the Owner Societies 2012

Published on 17 May 2012 on http://pubs.rsc.org | doi:10.1039/C2CP40944E
Downloaded by PNNL Technical Library on 25 June 2012

contain nitrogen and it is currently not possible to speciate the entire fraction of 0N compounds. However, the distinct CID signatures of aliphatic and heterocyclic NOC observed in this work enable more in-depth discussion about the formation of NOC products. Therefore, we focus on the possible formation pathways leading to the unexpected heterocyclic 2N products that accumulate during photolysis. As the concentrations of organic nitrates decrease from photolysis, and those for NO_3^- and NO_2^- do not, the source of 2N photoproducts in the irradiated SOA samples must be due primarily to the photolysis of organic nitrates, which are present at initially a factor of 100–1000 greater molar concentration than inorganic nitrogen ions.

Organic nitrates are known to photolyze mainly *via* three primary processes,[52,90,91] with the predominant pathway being the cleavage of the RO–NO_2 bond:

$$RONO_2 + h\nu \rightarrow RO + NO_2 \qquad (R1)$$

The NO_2 produced from photolysis may have the following photolytic fates in water:

$$NO_2 + h\nu\,(\lambda < 400\ \text{nm}) \rightarrow NO + O \qquad (R2)$$

$$NO_2 + h\nu\,(\lambda > 400\ \text{nm}) \rightarrow NO_2^* \qquad (R3)$$

Both reactions (2) and (3) are expected to be important, with a calculated $J_{NO_2} = 0.03\ s^{-1}$ and $0.02\ s^{-1}$, respectively, using gas-phase absorption cross sections,[92,93] quantum yields,[94] and the measured radiation flux from our lamps.

In water, the NO_2 radical may exist in equilibrium with its dimer N_2O_4. The dimer may disproportionate quickly in water to yield NO_3^- and NO_2^- ions.[95] At moderate NO_2 pressures ($p_{NO_2} < 1 \times 10^{-5}$ atm) the $[N_2O_4]/[NO_2]$ ratio is less than 0.02,[96] in good agreement with our IC analysis (Section 3.1) which shows that NO_3^- and NO_2^- ions are negligibly enhanced in the photolysis sample. The NO radical formed in reaction (2) can participate in autooxidation reactions in the presence of oxygen to form NO_2, N_2O_3, or NO_2^-.[97] HONO can also be introduced into solution in several ways: aqueous uptake onto aerosol water from the chamber experiments, NO_2^- equilibrium in solution, or NO oxidation by OH. If HONO is present, then the reactive NO^+ species is also available for nitrosation reaction.[98,99]

The product of reaction (3), NO_2*, is quickly quenched in solution. However, if NO_2* is formed in the immediate vicinity of an SOA molecule, it may react much faster than NO_2 with organics by H atom abstraction, addition, or electron transfer mechanisms to produce aldehydes, nitro (RNO_2) compounds, dinitro compounds, HONO, and other products,[91,95,100,101] although no evidence of heterocyclic N products have been reported from these reactions.

The 1,2-addition of oxidized nitrogen groups to alkenes may produce intermediates to furoxan-like molecules. We do not expect alkenes to be abundant in the initial composition due to the relatively complete oxidation of isoprene. Furthermore, the mass fraction of SOA compounds with positive AI, correlating to a non-zero number of C=C bonds, is 3–4% before photolysis. However the photochemical production of unsaturated hydrocarbons through Norrish II photochemistry (Section 3.1) may provide suitable alkenyl precursors for the formation of N-heterocyclic products. For example, the photolysis of one C_4 (or higher) carbonyl generates up to two alkenes with the Norrish II mechanism. As isoprene SOA compounds are initially large ($\langle C \rangle \sim 12$, Fig. 2a), the likelihood of Norrish II photochemistry should be high.

The aforementioned oxidized nitrogen species, stemming from the reaction of NO_2 and NO, in water that may participate in nitrosation of organics in the photolysis sample include N_2O_4, N_2O_3, and NO^+.[98] NO^+ will directly lead to nitrosation of alkenes; although the stepwise reaction may render the formation of vicinal dinitrogen groups uncompetitive. N_2O_4 and N_2O_3 (introduced into the solution by NO/O_2 system or NO_2^-/H_3O^+ system, respectively) will both react with alkenes in polar solvents to produce vicinal nitro-nitroso (R_1–$C(NO_2)$–$C(NO)R_2$) compounds[102–105] that ultimately lead to furoxans if there is sufficient acidity (pH $\sim$ 4) or oxidative conditions available for ring closure. However, the reaction is slow at room temperature (spanning several hours). Heat (*ca.* 100 °C) can also be used for the cyclization of vicinal dinitrogen compounds to form stable furoxans. However, these ring-closure conditions are not relevant to our experiments (Fig. S3b, ESI†). No available literature sources describe photochemical routes to the furoxan, from nitro-nitroso compounds or otherwise. We speculate this route has not been well-studied due to the relatively convenient alternative preparative routes to generate furoxans. It is possible that UV-visible radiation may accelerate the production of furoxans by generating more reactive intermediates, but this suggestion remains to be verified. Other types of compounds, *e.g.*, substituted ketones, may also be subject to nitrosation by N_2O_3 followed by intermolecular C–C coupling (at the nitro site) and subsequent ring closure to form furoxans.[106]

We note that the aforementioned reactions were studied under conditions not readily extrapolated to our experiments, *e.g.*, high nitrite concentrations or low pH. Furthermore, data are not available on the relative importance of each step and whether the rates of reaction can be enhanced through UV-visible irradiation. However, these nitrosation-promoting conditions and 2N heterocyclic formation should be more common in atmospheric droplets. Photoinduced nitrosation reactions in the atmosphere have been documented in the case of aromatic molecules.[107] The mechanism is not completely understood but the involvement of photo-produced NO_2 and NO is well-established. In this work, the role of photochemistry in the production of 2N heterocyclics is proposed, but future work is needed to obtain better understanding of the underlying mechanisms. Photochemically generated NO_x species from $RONO_2$ must play a role in product formation; however, there seems to be a missing mechanism for the observed ring closure. A possibility is that photochemical ring closure of dinitrogen intermediates traps the N compounds as a heterocycle; although relatively little is known about the aqueous photochemistry of organic nitrogen at this point to comment on the likelihood of this process. The hypothesis, however, is qualitatively consistent with the stable formation trends for 2N products during the continuous irradiation.

The exceptional stability of these furoxan-like heterocycles with respect to hydrolysis and UV irradiation[108] elevates their potential importance in atmospheric chemistry because they

Published on 17 May 2012 on http://pubs.rsc.org | doi:10.1039/C2CP40944E
Downloaded by PNNL Technical Library on 25 June 2012

may ultimately be organic nitrogen sinks in the atmosphere. For example, photolysis of benzofuroxan (λ = 366 nm)[109,110] and 3,4-dimethylfuroxan (λ = 254 nm)[111] produces the short-lived dinitroso intermediate that both thermally and photochemically regenerates the heterocycle. Comparatively, other photoproducts like carbonyls and nitro compounds are much more photolabile. Even if the formation of 2N heterocycles represents minor pathways compared to other organics, they may accumulate in substantial quantities in solution within the timescale of the photolysis experiments due to the stability of the aromatic 5-member ring. The sources for these long-lived pollutants in the atmosphere warrant further study as they may be formed under mildly photolytic conditions whenever the photoproduction of aqueous NO_x occurs in the presence of dissolved organics.

4. Conclusion and atmospheric significance

This work demonstrated that the composition of dissolved SOA may be significantly modified by solar radiation ($\sim$30% by mass after 4 h of photolysis in the lab roughly equivalent to 12 h photolysis in the atmosphere) and the effect of direct photolysis should not be ignored in studies of aqueous photochemistry. Furthermore, hydrolysis contributed a small but non-negligible loss pathway for some types of molecules, *e.g.*, organic nitrates. The composition changes are observed within 1 h photolysis (up to 3 h in the atmosphere), which is on the order of the lifetime of clouds, water films on environmental surfaces, and hydrated SOA. The presence of a large amount of ultrafine aerosols can further promote the formation of photoproducts in clouds due to both increasing the lifetime of clouds[112] and increase the concentration of dissolved OM.

The tentative identification of furoxan-like compounds in our work is the first association of these types of molecules with organic aerosols and the first report of the photochemical production of N heterocycles in cloud processing of SOA. Furoxans are typically researched as potential drugs as they are nitrogen oxide donors.[108] As such, the presence of the bound N=O moiety in SOA material may have a large potential for bioactivity. N-heterocycles based on the 5-member imidazole or the 6-member pyridine and their derivatives have only recently been recognized as important components in atmospheric OM from their association with brown carbon[113,114] and biomass burning OA.[86] The detection of abundant signal from molecules with C–N bonds in ambient aerosols from urban atmospheres, which are not associated with oxidation chemistry,[115] lend further support that reactions producing N-heterocycles may be more prevalent in nature than currently realized.

Our study discussed possible aqueous pathways to the formation of N-heterocycles from compounds commonly found in SOA. The 19% upper limit yield of 2N photoproducts in this work is unexpectedly large and it is reasonable to conclude that a photochemical mechanism for 2N heterocyclics is still undiscovered. However, the known conditions that may promote heterocyclic furoxan production are vastly more common in the atmosphere than in our experiments, as high concentrations of NO_2^-, NO_3^-, acidity, oxidants and dissolved organic compounds can be found in cloud/fog droplets and wet aerosol. Therefore atmospheric water samples should be closely examined with HR-MS techniques for heterocyclic nitrogen. The conversion of aliphatic organic nitrates to photostable 2N heterocyclics has important implications for the nitrogen budget in the atmosphere. There are still large gaps in the collective knowledge of atmospheric aqueous photochemistry, but it is clear that direct photolysis can be important for many classes of compounds and ambient conditions.

Acknowledgements

The UCI group gratefully acknowledges support by the NSF grants ATM-0831518 and CHE-0909227. The PNNL group acknowledges support provided by the intramural research and development program of the W. R. Wiley Environmental Molecular Sciences Laboratory (EMSL), a national scientific user facility sponsored by the Office of Biological and Environmental Research and located at PNNL. PNNL is operated for the U.S. Department of Energy by Battelle Memorial Institute under contract no. DE-AC06-76RL0 1830. We also wish to acknowledge the director of the UCI Urban Water Research Center, Dr William J. Cooper, for the use of the ion chromatography instrument and Linda Tseng and Dr Jean Elkoury of the UCI Department of Environmental Engineering for useful discussions.

References

1 B. Verheggen, J. Cozic, E. Weingartner, K. Bower, S. Mertes, P. Connolly, M. Gallagher, M. Flynn, T. Choularton and U. Baltensperger, *J. Geophys. Res.*, 2007, **112**, D23202.
2 S. Henning, S. Bojinski, K. Diehl, S. Ghan, S. Nyeki, E. Weingartner, S. Wurzler and U. Baltensperger, *Geophys. Res. Lett.*, 2004, **31**, L06101.
3 M. C. Facchini, S. Fuzzi, S. Zappoli, A. Andracchio, A. Gelencsér, G. Kiss, Z. Krivácsy, E. Mészáros, H.-C. Hansson, T. Alsberg and Y. Zebühr, *J. Geophys. Res.*, 1999, **104**, 26821–26832.
4 C. Hoose, U. Lohmann, R. Bennartz, B. Croft and G. Lesins, *Atmos. Chem. Phys.*, 2008, **8**, 6939–6963.
5 A. J. Prenni, M. D. Petters, S. M. Kreidenweis, P. J. DeMott and P. J. Ziemann, *J. Geophys. Res.*, 2007, **112**, D10223.
6 A. E. Gomez, H. Wortham, R. Strekowski, C. Zetzsch and S. Gligorovski, *Environ. Sci. Technol.*, 2012, **46**, 1955–1963.
7 A. Jammoul, S. Gligorovski, C. George and B. D'Anna, *J. Phys. Chem. A*, 2008, **112**, 1268–1276.
8 E. C. Minerath, M. P. Schultz and M. J. Elrod, *Environ. Sci. Technol.*, 2009, **43**, 8133–8139.
9 K. S. Hu, A. I. Darer and M. J. Elrod, *Atmos. Chem. Phys.*, 2011, **11**, 8307–8320.
10 T. B. Nguyen, P. B. Lee, K. M. Updyke, D. L. Bones, J. Laskin, A. Laskin and S. A. Nizkorodov, *J. Geophys. Res.*, 2012, **117**, D01207.
11 H. R. Pruppacher and R. Jaenicke, *Atmos. Res.*, 1995, **38**, 283–295.
12 B. Lin and W. B. Rossow, *J. Clim.*, 1996, **9**, 2890–2902.
13 P. J. G. Rehbein, C.-H. Jeong, M. L. McGuire, X. Yao, J. C. Corbin and G. J. Evans, *Environ. Sci. Technol.*, 2011, **45**, 4346–4352.
14 Y. B. Lim, Y. Tan, M. J. Perri, S. P. Seitzinger and B. J. Turpin, *Atmos. Chem. Phys.*, 2010, **10**, 10521–10539.
15 B. Ervens, B. J. Turpin and R. J. Weber, *Atmos. Chem. Phys.*, 2011, **11**, 11069–11102.
16 A. G. Rincon, M. I. Guzman, M. R. Hoffmann and A. J. Colussi, *J. Phys. Chem. Lett.*, 2010, **1**, 368–373.
17 J. L. Chang and J. E. Thompson, *Atmos. Environ.*, 2010, **44**, 541–551.
18 L. Yao, T. Tritscher, A. P. Praplan, P. F. DeCarlo, B. Temime-Roussel, E. Quivet, N. Marchand, J. Dommen, U. Baltensperger and A. Monod, *Atmos. Chem. Phys. Discuss.*, 2011, **11**, 21489–21532.

 This journal is © the Owner Societies 2012

View Online

Published on 17 May 2012 on http://pubs.rsc.org | doi:10.1039/C2CP40944E
Downloaded by PNNL Technical Library on 25 June 2012

19 A. Albinet, C. Minero and D. Vione, *Chemosphere*, 2010, **80**, 753–758.
20 A. K. Y. Lee, R. Zhao, S. S. Gao and J. P. D. Abbatt, *J. Phys. Chem. A*, 2011, **115**, 10517–10526.
21 Y. Tan, M. J. Perri, S. P. Seitzinger and B. J. Turpin, *Environ. Sci. Technol.*, 2009, **43**, 8105–8112.
22 A. G. Carlton, B. J. Turpin, K. E. Altieri, S. Seitzinger, A. Reff, H.-J. Lim and B. Ervens, *Atmos. Environ.*, 2007, **41**, 7588–7602.
23 Y. Tan, A. G. Carlton, S. P. Seitzinger and B. J. Turpin, *Atmos. Environ.*, 2010, **44**, 5218–5226.
24 K. E. Altieri, S. P. Seitzinger, A. G. Carlton, B. J. Turpin, G. C. Klein and A. G. Marshall, *Atmos. Environ.*, 2008, **42**, 1476–1490.
25 K. E. Altieri, A. G. Carlton, H. J. Lim, B. J. Turpin and S. P. Seitzinger, *Environ. Sci. Technol.*, 2006, **40**, 4956–4960.
26 A. G. Carlton, B. J. Turpin, H. J. Lim, K. E. Altieri and S. Seitzinger, *Geophys. Res. Lett.*, 2006, **33**, L06822.
27 M. I. Guzman, A. J. Colussi and M. R. Hoffmann, *J. Phys. Chem. A*, 2006, **110**, 3619–3626.
28 M. J. Perri, S. Seitzinger and B. J. Turpin, *Atmos. Environ.*, 2009, **43**, 1487–1497.
29 A. K. Y. Lee, P. Herckes, W. R. Leaitch, A. M. Macdonald and J. P. D. Abbatt, *Geophys. Res. Lett.*, 2011, **38**, L11805.
30 S. A. Nizkorodov, J. Laskin and A. Laskin, *Phys. Chem. Chem. Phys.*, 2011, **13**, 3612–3629.
31 J. Laskin, A. Laskin, P. J. Roach, G. W. Slysz, G. A. Anderson, S. A. Nizkorodov, D. L. Bones and L. Q. Nguyen, *Anal. Chem. (Washington, DC, U. S.)*, 2010, **82**, 2048–2058.
32 J. L. Collett, P. Herckes, S. Youngster and T. Lee, *Atmos. Res.*, 2008, **87**, 232–241.
33 J. L. Collett, A. Bator, D. E. Sherman, K. F. Moore, K. J. Hoag, B. B. Demoz, X. Rao and J. E. Reilly, *Atmos. Res.*, 2002, **64**, 29–40.
34 A. Cappiello, E. De Simoni, C. Fiorucci, F. Mangani, P. Palma, H. Trufelli, S. Decesari, M. C. Facchini and S. Fuzzi, *Environ. Sci. Technol.*, 2003, **37**, 1229–1240.
35 P. D. Capel, R. Gunde, F. Zuercher and W. Giger, *Environ. Sci. Technol.*, 1990, **24**, 722–727.
36 P. Herckes, T. Lee, L. Trenary, G. Kang, H. Chang and J. L. Collett, *Environ. Sci. Technol.*, 2002, **36**, 4777–4782.
37 P. Herckes, H. Chang, T. Lee and J. Collett, *Water Air Soil Pollut.*, 2007, **181**, 65–75.
38 D. J. Jacob, J. M. Waldman, J. W. Munger and M. R. Hoffmann, *Tellus, Ser. B*, 1984, **36**, 272–285.
39 S. Fuzzi, M. C. Facchini, S. Decesari, E. Matta and M. Mircea, *Atmos. Res.*, 2002, **64**, 89–98.
40 J. Fisak, M. Tesar, D. Rezacova, V. Elias, V. Weignerova and D. Fottova, *Atmos. Res.*, 2002, **64**, 75–87.
41 R. G. Zepp, J. Hoigne and H. Bader, *Environ. Sci. Technol.*, 1987, **21**, 443–450.
42 A. Torrents, B. G. Anderson, S. Bilboulian, W. E. Johnson and C. J. Hapeman, *Environ. Sci. Technol.*, 1997, **31**, 1476–1482.
43 R. K. Talukdar, J. B. Burkholder, M. Hunter, M. K. Gilles, J. M. Roberts and A. R. Ravishankara, *J. Chem. Soc., Faraday Trans.*, 1997, **93**, 2797–2805.
44 J. M. Roberts and R. W. Fajer, *Environ. Sci. Technol.*, 1989, **23**, 945–951.
45 I. Barnes, K. H. Becker and T. Zhu, *J. Atmos. Chem.*, 1993, **17**, 353–373.
46 W. T. Luke, R. R. Dickerson and L. J. Nunnermacker, *J. Geophys. Res.*, 1989, **94**, 14905–14921.
47 R. Volkamer, P. Spietz, J. Burrows and U. Platt, *J. Photochem. Photobiol., A*, 2005, **172**, 35–46.
48 C. Bacher, G. S. Tyndall and J. J. Orlando, *J. Atmos. Chem.*, 2001, **39**, 171–189.
49 Y. Q. Chen, W. J. Wang and L. Zhu, *J. Phys. Chem. A*, 2000, **104**, 11126–11131.
50 Y. Q. Chen and L. Zhu, *J. Phys. Chem. A*, 2003, **107**, 4643–4651.
51 A. Horowitz, R. Meller and G. K. Moortgat, *J. Photochem. Photobiol., A*, 2001, **146**, 19–27.
52 J. G. Calvert and J. N. Pitts, *Photochemistry*, John Wiley & Sons, New York-London-Sydney, 1966, 899 pp.
53 Y. L. Sun, Q. Zhang, C. Anastasio and J. Sun, *Atmos. Chem. Phys.*, 2010, **10**, 4809–4822.
54 A. P. Bateman, S. A. Nizkorodov, J. Laskin and A. Laskin, *Phys. Chem. Chem. Phys.*, 2011, **13**, 12199–12212.
55 A. Monod, E. Chevallier, J. R. Durand, J. F. Doussin, B. Picquet-Varrault and P. Carlier, *Atmos. Environ.*, 2007, **41**, 2412–2426.
56 B. Ervens, S. Gligorovski and H. Herrmann, *Phys. Chem. Chem. Phys.*, 2003, **5**, 1811–1824.
57 C. Anastasio and K. G. McGregor, *Atmos. Environ.*, 2001, **35**, 1079–1089.
58 B. Ervens, C. George, J. E. Williams, G. V. Buxton, G. A. Salmon, M. Bydder, F. Wilkinson, F. Dentener, P. Mirabel, R. Wolke and H. Herrmann, *J. Geophys. Res.*, 2003, **108**, 4426.
59 D. J. Jacob, *J. Geophys. Res.*, 1986, **91**, 9807–9826.
60 J. D. Fuentes, M. Lerdau, R. Atkinson, D. Baldocchi, J. W. Bottenheim, P. Ciccioli, B. Lamb, C. Geron, L. Gu, A. Guenther, T. D. Sharkey and W. Stockwell, *Bull. Am. Meteorol. Soc.*, 2000, **81**, 1537–1575.
61 A. Guenther, T. Karl, P. Harley, C. Wiedinmyer, P. I. Palmer and C. Geron, *Atmos. Chem. Phys.*, 2006, **6**, 3181–3210.
62 J. D. Surratt, S. M. Murphy, J. H. Kroll, N. L. Ng, L. Hildebrandt, A. Sorooshian, R. Szmigielski, R. Vermeylen, W. Maenhaut, M. Claeys, R. C. Flagan and J. H. Seinfeld, *J. Phys. Chem. A*, 2006, **110**, 9665–9690.
63 R. Szmigielski, J. D. Surratt, R. Vermeylen, K. Szmigielska, J. H. Kroll, N. L. Ng, S. M. Murphy, A. Sorooshian, J. H. Seinfeld and M. Claeys, *J. Mass Spectrom.*, 2007, **42**, 101–116.
64 G. Werner, J. Kastler, R. Looser and K. Ballschmiter, *Angew. Chem., Int. Ed.*, 1999, **38**, 1634–1637.
65 F. Paulot, J. D. Crounse, H. G. Kjaergaard, J. H. Kroll, J. H. Seinfeld and P. O. Wennberg, *Atmos. Chem. Phys.*, 2009, **9**, 1479–1501.
66 E. O. Edney, T. E. Kleindienst, M. Jaoui, M. Lewandowski, J. H. Offenberg, W. Wang and M. Claeys, *Atmos. Environ.*, 2005, **39**, 5281–5289.
67 T. B. Nguyen, P. J. Roach, J. Laskin, A. Laskin and S. A. Nizkorodov, *Atmos. Chem. Phys.*, 2011, **11**, 6931–6944.
68 T. B. Nguyen, J. Laskin, A. Laskin and S. A. Nizkorodov, *Environ. Sci. Technol.*, 2011, **45**, 6908–6918.
69 X. Tie, S. Madronich, S. Walters, R. Zhang, P. Rasch and W. Collins, *J. Geophys. Res.*, 2003, **108**, 4642.
70 T. B. Nguyen, A. P. Bateman, D. L. Bones, S. A. Nizkorodov, J. Laskin and A. Laskin, *Atmos. Environ.*, 2010, **44**, 1032–1042.
71 T. Kind and O. Fiehn, *BMC Bioinf.*, 2006, **7**, 234.
72 T. B. Nguyen, S. A. Nizkorodov, A. Laskin and J. Laskin, *Anal. Methods*, 2012, submitted.
73 K. S. Docherty, W. Wu, Y. B. Lim and P. J. Ziemann, *Environ. Sci. Technol.*, 2005, **39**, 4049–4059.
74 B. P. Koch and T. Dittmar, *Rapid Commun. Mass Spectrom.*, 2006, **20**, 926–932.
75 T. Brinkmann, P. Horsch, D. Sartorius and F. H. Frimmel, *Environ. Sci. Technol.*, 2003, **37**, 4190–4198.
76 E. B. Kujawinski, R. Del Vecchio, N. V. Blough, G. C. Klein and A. G. Marshall, *Mar. Chem.*, 2004, **92**, 23–37.
77 Y. Sun, Q. Zhang, A. M. Macdonald, K. Hayden, S. M. Li, J. Liggio, P. S. K. Liu, K. G. Anlauf, W. R. Leaitch, A. Steffen, M. Cubison, D. R. Worsnop, A. van Donkelaar and R. V. Martin, *Atmos. Chem. Phys.*, 2009, **9**, 3095–3111.
78 A. C. Aiken, P. F. Decarlo, J. H. Kroll, D. R. Worsnop, J. A. Huffman, K. S. Docherty, I. M. Ulbrich, C. Mohr, J. R. Kimmel, D. Sueper, Y. Sun, Q. Zhang, A. Trimborn, M. Northway, P. J. Ziemann, M. R. Canagaratna, T. B. Onasch, M. R. Alfarra, A. S. H. Prevot, J. Dommen, J. Duplissy, A. Metzger, U. Baltensperger and J. L. Jimenez, *Environ. Sci. Technol.*, 2008, **42**, 4478–4485.
79 A. C. Aiken, D. Salcedo, M. J. Cubison, J. A. Huffman, P. F. DeCarlo, I. M. Ulbrich, K. S. Docherty, D. Sueper, J. R. Kimmel, D. R. Worsnop, A. Trimborn, M. Northway, E. A. Stone, J. J. Schauer, R. M. Volkamer, E. Fortner, B. de Foy, J. Wang, A. Laskin, V. Shutthanandan, J. Zheng, R. Zhang, J. Gaffney, N. A. Marley, G. Paredes-Miranda, W. P. Arnott, L. T. Molina, G. Sosa and J. L. Jimenez, *Atmos. Chem. Phys.*, 2009, **9**, 6633–6653.
80 Y. L. Sun, Q. Zhang, J. J. Schwab, K. L. Demerjian, W. N. Chen, M. S. Bae, H. M. Hung, O. Hogrefe, B. Frank, O. V. Rattigan and Y. C. Lin, *Atmos. Chem. Phys.*, 2011, **11**, 1581–1602.
81 K. E. Kautzman, J. D. Surratt, M. N. Chan, A. W. H. Chan, S. P. Hersey, P. S. Chhabra, N. F. Dalleska, P. O. Wennberg,

View Online

R. C. Flagan and J. H. Seinfeld, *J. Phys. Chem. A*, 2009, **114**, 913–934.
82 J. M. Roberts, *Atmos. Environ.*, 1990, **24**, 243–287.
83 A. W. H. Chan, M. N. Chan, J. D. Surratt, P. S. Chhabra, C. L. Loza, J. D. Crounse, L. D. Yee, R. C. Flagan, P. O. Wennberg and J. H. Seinfeld, *Atmos. Chem. Phys.*, 2010, **10**, 7169–7188.
84 E. P. L. Hunter and S. G. Lias, *J. Phys. Chem. Ref. Data*, 1998, **27**, 413–656.
85 R. G. W. Norrish and C. H. Bamford, *Nature*, 1937, **140**, 195–196.
86 A. Laskin, J. S. Smith and J. Laskin, *Environ. Sci. Technol.*, 2009, **43**, 3764–3771.
87 J. V. R. Kaufman and J. P. Picard, *Chem. Rev. (Washington, DC, U. S.)*, 1959, **59**, 429–461.
88 K. Levsen, H. M. Schiebel, J. K. Terlouw, K. J. Jobst, M. Elend, A. Preib, H. Thiele and A. Ingendoh, *J. Mass Spectrom.*, 2007, **42**, 1024–1044.
89 D. G. I. Kingston, B. W. Hobrock, M. M. Bursey and J. T. Bursey, *Chem. Rev. (Washington, DC, U. S.)*, 1975, **75**, 693–730.
90 R. E. Rebbert, *J. Phys. Chem.*, 1963, **67**, 1923–1925.
91 J. A. Gray and D. W. G. Style, *Trans. Faraday Soc.*, 1953, **49**, 52–57.
92 A. C. Vandaele, C. Hermans, P. C. Simon, M. Carleer, R. Colin, S. Fally, M. F. Merienne, A. Jenouvrier and B. Coquart, *J. Quant. Spectrosc. Radiat. Transfer*, 1998, **59**, 171–184.
93 W. Schneider, G. K. Moortgat, G. S. Tyndall and J. P. Burrows, *J. Photochem. Photobiol., A*, 1987, **40**, 195–217.
94 J. Troe, *Z. Physiol. Chem.*, 2000, **214**, 573–581.
95 R. E. Huie, *Toxicology*, 1994, **89**, 193–216.
96 Y. N. Lee and S. E. Schwartz, *J. Phys. Chem.*, 1981, **85**, 840–848.
97 R. S. Lewis and W. M. Deen, *Chem. Res. Toxicol.*, 1994, **7**, 568–574.
98 D. H. L. Williams, *Nitrosation*, Cambridge University Press, Cambridge, UK, 1988, 214 pp.
99 D. A. Wink, J. F. Darbyshire, R. W. Nims, J. E. Saavedra and P. C. Ford, *Chem. Res. Toxicol.*, 1993, **6**, 23–27.
100 M. E. Umstead, S. A. Lloyd, J. W. Fleming and M. C. Lin, *Appl. Phys. B: Lasers Opt.*, 1985, **38**, 219–224.
101 M. E. Umstead and M. C. Lin, *Appl. Phys. B: Lasers Opt.*, 1986, **39**, 61–63.
102 A. S. Demir and H. Findik, *Lett. Org. Chem.*, 2005, **2**, 602–604.
103 C. Velazquez, P. N. P. Rao, R. McDonald and E. E. Knaus, *Bioorg. Med. Chem.*, 2005, **13**, 2749–2757.
104 A. Napolitano and M. d'Ischia, *J. Org. Chem.*, 2002, **67**, 803–810.
105 R. Calvino, B. Ferrarotti, A. Serafino and A. Gasco, *Heterocycles*, 1985, **23**, 1955–1960.
106 W. F. Nirode, J. M. Luis, J. F. Wicker and N. M. Wachter, *Bioorg. Med. Chem. Lett.*, 2006, **16**, 2299–2301.
107 P. Boule, D. W. Bahnemann and P. K. Robertson, *Environmental photochemistry*, Springer-Verlag, Berlin/Heidelberg, 1999, 365 pp.
108 H. Cerecetto, M. Gonzalez and M. Khan, *Benzofuroxan and furoxan. Chemistry and biology of bioactive heterocycles IV*, Springer, Berlin/Heidelberg, 2007, vol. 10, pp. 265–308.
109 N. P. Hacker, *J. Org. Chem.*, 1991, **56**, 5216–5217.
110 S. Murata and H. Tomioka, *Chem. Lett.*, 1992, 57–60.
111 H.-J. r. Himmel, S. Konrad, W. Friedrichsen and G. Rauhut, *J. Phys. Chem. A*, 2003, **107**, 6731–6737.
112 S. Solomon, D. Qin, M. Manning, Z. Chen, M. Marquis, K. B. Averyt, M. Tignor and H. L. Miller, *Climate Change 2007: The Physical Science Basis. Contribution of Working Group I to the Fourth Assessment Report of the Intergovernmental Panel on Climate Change*, IPCC, 2007.
113 D. O. De Haan, M. A. Tolbert and J. L. Jimenez, *Geophys. Res. Lett.*, 2009, **36**, L11819.
114 D. O. De Haan, L. N. Hawkins, J. A. Kononenko, J. J. Turley, A. L. Corrigan, M. A. Tolbert and J. L. Jimenez, *Environ. Sci. Technol.*, 2011, **45**, 984–991.
115 X. F. Wang, S. Gao, X. Yang, H. Chen, J. M. Chen, G. S. Zhuang, J. D. Surratt, M. N. Chan and J. H. Seinfeld, *Environ. Sci. Technol.*, 2010, **44**, 4441–4446.

Published on 17 May 2012 on http://pubs.rsc.org | doi:10.1039/C2CP40944E
Downloaded by PNNL Technical Library on 25 June 2012

 This journal is © the Owner Societies 2012